2013 IEEE/RSJ International Conference on
Intelligent Robots and Systems (IROS)
November 3-7, 2013. Tokyo, Japan

Characterizing and Addressing Dynamic Singularities in the Time-Optimal Path Parameterization Algorithm

Quang-Cuong Pham*

***Abstract*— The algorithm for finding the time-optimal parameterization of a given path subject to dynamics constraints developed mostly in the 80's and 90's plays a central role in a number of important robotic theories and applications. A critical issue in its implementation is associated with the so-called dynamic singularities, i.e. the points where the maximum velocity curve is continuous but undifferentiable and where the minimum and maximum accelerations are not naturally defined. Since such singularities arise in most real-world problem instances, characterizing and addressing them appropriately is of particular interest. Yet, from original articles to reference textbooks, this has not yet been done completely correctly. The contribution of the present article is two-fold. First, we derive a complete characterization of dynamic singularities. In particular, we show that not all zero-inertia points are dynamically singular. Second, we suggest how to appropriately address these singularities. In particular, we derive the analytic expressions of the correct optimal backward and forward accelerations from such points.**

I. INTRODUCTION

The algorithm for finding the Time-Optimal Parameterization of a given Path (TOPP) subject to dynamics constraints developed in the 80's and 90's [1], [2], [3], [4], [5], [6] plays a central role in a number of important theories and applications in the field of robotics. Initially developed for robotic manipulators subject to torque limits, it has been subsequently extended to many other types of systems and constraints, such as manipulators with gripper and payload constraints [7], vehicles with friction constraints [8], humanoid robots with joint velocity and acceleration limits [9] or ZMP constraints [10]. From a theoretical viewpoint, it serves as the foundation upon which several *global* (i.e. when the path is not fixed) planning algorithms have been developed [11], [12], [13], [14].

A critical issue in the implementation of the TOPP algorithm is associated with the so-called *dynamic singularities* [1], i.e. the points where the maximum velocity curve is continuous but undifferentiable and where the minimum and maximum accelerations are not naturally defined (for more details, see section II). Since such singularities arise in most real-world problem instances [6], characterizing and addressing them appropriately is of particular interest. Yet, in most references devoted to the TOPP algorithm, from the original articles [3], [4], [5], [6], [9] to reference textbooks [16], this has not yet been done completely correctly.

*School of Mechanical & Aerospace Engineering, Nanyang Technological University, Singapore. Email: cuong.pham@normalesup.org.

[1]The term "dynamic singularity" must be understood here in the sense of [5], which is different from that used in a completely different context by [15].

In section II, we briefly review the TOPP algorithm and highlight the difficulties associated with dynamic singularities. We also outline our proposed solution and, in the process, establish a general classification of switch points and related notions.

Next, we detail the technical contributions of the article:

- In section III, we derive a complete *characterization* of the dynamic singularities. In particular, we show that, contrary to the statements of [3], [4], [5], [6], [16], [9], *not all* zero-inertia points constitute dynamic singularities. Furthermore, we show that there are in fact two different types of dynamic singularities.
- In section IV, we suggest how to appropriately *address* the two types of dynamic singularities. In particular, we derive the analytic expressions of the optimal backward and forward accelerations from such points, which differ from the ones proposed in [5], [6].

Finally, in section V, we conclude by summarizing and discussing the obtained results and possible extensions.

II. BACKGROUND ON THE TOPP ALGORITHM

A. Review of the Core Algorithm

Consider an n-dof manipulator with dynamics equation

$$\mathbf{M}(\mathbf{q})\ddot{\mathbf{q}} + \dot{\mathbf{q}}^\top \mathbf{C}(\mathbf{q})\dot{\mathbf{q}} + \mathbf{g}(\mathbf{q}) = \tau, \tag{1}$$

where $\mathbf{q}$ is a $n \times 1$ vector of joint values, $\mathbf{M}$ the $n \times n$ manipulator inertia matrix, $\mathbf{C}$ the $n \times n \times n$ Coriolis tensor, $\mathbf{g}$ the $n \times 1$ vector of gravity forces and τ the $n \times 1$ vector of actuator torques. Assume that this manipulator is subject to the torque limits of the form: for every joint $i \in [1, n]$ and time u

$$\tau_i^{\min} \leq \tau_i(u) \leq \tau_i^{\max}. \tag{2}$$

Consider now a path P – represented as the underlying path of a trajectory $\mathbf{q}(s)_{s\in[0,T]}$ – in the manipulator configuration space. We assume that $\mathbf{q}(s)_{s\in[0,T]}$ is C^1- and piecewise C^2-continuous. The TOPP algorithm, which we summarize and reformulate below, allows to find the fastest time-parameterization of P starting from a given velocity v_{beg} and ending at a given velocity v_{end} while respecting the torque limits. More precisely, a *time-parameterization* of P – or a time-*re*parameterization of $\mathbf{q}(s)_{s\in[0,T]}$ – is an increasing *function* $s : [0, T'] \to [0, T]$. Differentiating $\mathbf{q}(s(t))$ with respect to t yields

$$\dot{\mathbf{q}} = \mathbf{q}_s \dot{s}, \quad \ddot{\mathbf{q}} = \mathbf{q}_s \ddot{s} + \mathbf{q}_{ss} \dot{s}^2, \tag{3}$$

where $\mathbf{q}_s = \frac{\mathrm{d}\mathbf{q}}{\mathrm{d}s}$ and $\mathbf{q}_{ss} = \frac{\mathrm{d}^2\mathbf{q}}{\mathrm{d}s^2}$. Substituting (3) into (1) then

leads to

$$\mathbf{M}(\mathbf{q})(\mathbf{q}_s\ddot{s} + \mathbf{q}_{ss}\dot{s}^2) + \mathbf{q}_s^\top \mathbf{C}(\mathbf{q})\mathbf{q}_s\dot{s}^2 + \mathbf{g}(\mathbf{q}) = \tau(s). \quad (4)$$

The above equation can be rewritten in the following form

$$\mathbf{a}(s)\ddot{s} + \mathbf{b}(s)\dot{s}^2 + \mathbf{c}(s) = \tau(s), \quad \text{where}$$

$$\begin{aligned} \mathbf{a}(s) &= \mathbf{M}(\mathbf{q}(s))\mathbf{q}_s(s), \\ \mathbf{b}(s) &= \mathbf{M}(\mathbf{q}(s))\mathbf{q}_{ss}(s) + \mathbf{q}_s(s)^\top \mathbf{C}(\mathbf{q}(s))\mathbf{q}_s(s), \\ \mathbf{c}(s) &= \mathbf{g}(\mathbf{q}(s)). \end{aligned}$$

The torque limits of (2) can now be expressed by the following $2n$ inequalities: for every $i \in [1, n]$

$$\tau_i^{\min} \leq a_i(s)\ddot{s} + b_i(s)\dot{s}^2 + c_i(s) \leq \tau_i^{\max}.$$

Next, if $a_i(s) \neq 0$ (the case $a_i = 0$ corresponds to a *zero-inertia* point, whose treatment is the topic of the present paper, see section II-B), one can write

$$\alpha_i(s, \dot{s}) \leq \ddot{s} \leq \beta_i(s, \dot{s}), \quad \text{with}$$

$$\begin{aligned} \alpha_i(s, \dot{s}) &= (\tau_i^\alpha - b_i(s)\dot{s}^2 - c_i(s))/a_i(s), \\ \beta_i(s, \dot{s}) &= (\tau_i^\beta - b_i(s)\dot{s}^2 - c_i(s))/a_i(s), \end{aligned}$$

where τ_i^α and τ_i^β are defined by

$$\begin{cases} \tau_i^\alpha = \tau_i^{\min};\ \tau_i^\beta = \tau_i^{\max} & \text{if } a_i(s) > 0, \\ \tau_i^\alpha = \tau_i^{\max};\ \tau_i^\beta = \tau_i^{\min} & \text{if } a_i(s) < 0. \end{cases}$$

Thus $\ddot{s}$ is bounded as follows

$$\alpha(s, \dot{s}) \leq \ddot{s} \leq \beta(s, \dot{s}), \quad (5)$$

where $\alpha(s, \dot{s}) = \max_i \alpha_i(s, \dot{s})$ and $\beta(s, \dot{s}) = \min_i \beta_i(s, \dot{s})$.

Note that $(s, \dot{s}) \mapsto (\dot{s}, \alpha(s, \dot{s}))$ and $(s, \dot{s}) \mapsto (\dot{s}, \beta(s, \dot{s}))$ can be seen as two vector fields in the $(s, \dot{s})$ plane. One can integrate velocity profiles following the field $(\dot{s}, \alpha(s, \dot{s}))$ (from now on, α in short) to obtain *minimum acceleration* profiles (or α-profiles), or following the field β to obtain *maximum acceleration* profiles (or β-profiles).

Next, observe that if $\alpha(s, \dot{s}) > \beta(s, \dot{s})$ then, from (5), there is no possible value for $\ddot{s}$. Thus, to be valid, any velocity profile must stay below the maximum velocity curve (MVC in short) defined by

$$\mathrm{MVC}(s) = \begin{cases} \min\{\dot{s} \geq 0 : \alpha(s, \dot{s}) = \beta(s, \dot{s})\} & \text{if } \alpha(s, 0) < \beta(s, 0), \\ 0 & \text{if } \alpha(s, 0) \geq \beta(s, 0). \end{cases}$$

It was shown (see e.g. [5]) that the time-minimal velocity profile is obtained by a *bang-bang*-type control, i.e., whereby the optimal profile follows alternatively the β and α fields while always staying below the MVC. More precisely, the algorithm is as follows:

1) In the $(s, \dot{s})$ plane, start from $(s = 0, \dot{s} = v_{\mathrm{beg}}/\|\mathbf{q}_s(0)\|)$ and integrate forward following β until hitting either
   (i) the MVC, in this case go to step 2;
   (ii) the horizontal line $\dot{s} = 0$, in this case the path is not dynamically traversable;
   (iii) the vertical line $s = s_{\mathrm{end}}$, in this case go to step 3.
2) Search forward along the MVC for the next candidate $\alpha \to \beta$ switch point (cf. section II-B). From such a switch point:
   a) integrate *backward* following α, until *intersecting* a forward β-profile (from step 1 or recursively from the current step 2). The intersection point constitutes a $\beta \to \alpha$ switch point;
   b) integrate *forward* following β. Then continue as in step 1.

   The resulting forward profile will be the concatenation of the intersected forward β-profile, the backward α-profile obtained in (a), and the forward β-profile obtained in (b).
3) Start from $(s = s_{\mathrm{end}}, \dot{s} = v_{\mathrm{end}}/\|\mathbf{q}_s(s_{\mathrm{end}})\|)$ and integrate *backward* following α, until intersecting a forward profile obtained in steps 1 or 2. The intersection point constitutes a $\beta \to \alpha$ switch point. The final profile will be the concatenation of the intersected forward profile and the backward α-profile just computed.

B. A New Classification of Switch Points

It was shown in [3], [4], [5], [6] that a given point s is a candidate $\alpha \to \beta$ switch point only in the following three cases:

- the MVC is *discontinuous* at s. In this case, if s is indeed a switch point, it is labeled as "discontinuous";
- the MVC is *continuous* but *undifferentiable* at s. In this case, if s is indeed a switch point, then it is labeled as "undifferentiable" (previous works labeled such a switch point as a "zero-inertia point" [4] or as a "critical/singular point" [5], [6]; however we shall see below that such terminologies are ambiguous);
- the MVC is *continuous* and *differentiable* at s and the *tangent vector* to the MVC at $(s, \mathrm{MVC}(s))$ is collinear with the vector $(\mathrm{MVC}(s), \alpha(s, \mathrm{MVC}(s)))$ [or, which is the same since we are on the MVC, collinear with the vector $(\mathrm{MVC}(s), \beta(s, \mathrm{MVC}(s)))$]. In this case, if s is indeed a switch point, it is labeled as "tangent".

Characterizing discontinuous (respectively, tangent) switch points does not involve particular difficulties since it suffices to construct the MVC and examine whether it is discontinuous (respectively, whether the tangent to the MVC is collinear with α) for all discretized points s along the path. Regarding the undifferentiable switch points, one approach could consist of checking whether the MVC is continuous but undifferentiable at s. However, this approach is seldom used in the literature since it is comparatively more prone to discretization errors. Instead, it was proposed (cf. [3], [4], [5], [16], [9]) to equate undifferentiable points with *zero-inertia points*, i.e. the points s where $a_k(s) = 0$ for one of the joints k, and to consequently search for zero-inertia points. However, this method is not correct: we shall indeed show in section III that *not all zero-inertia points are undifferentiable*.

It can be conversely noted that *not all undifferentiable points are caused by zero-inertia*. This case occurs for instance at s^* where the α (or β) on the MVC is given by α_i for $s < s^*$ and by α_j, $j \neq i$, for $s > s^*$. Note that, as for discontinuous and tangent points, this type of undifferentiable points does not involve particular

difficulties since α and β are well-defined at s^* (there is no division by 0). In practice, we have never encountered such undifferentiable points that indeed constitute switch points: the α ($= \beta$) vector always "traverses" the MVC at such points.

Finally, undifferentiable points caused by zero-inertia properly constitute *dynamic singularities*. We shall show that they are in fact of *two different types*, which we call respectively of *type I* and of *type II*, and which can give rise to two different types of undifferentiable switch points (cf. section III).

In light of the above discussion, a general classification of switch points and related notions can be given as in Fig. 1.

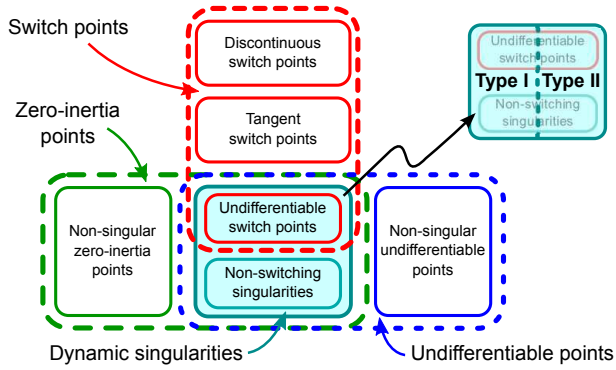

Fig. 1. Classification of switch points and related notions.

C. Previous and New Solutions to Dynamic Singularities

The next difficulty consists in the selection of the optimal acceleration to initiate the backward and forward integrations from a dynamic singularity s^*: indeed the fields α and β are not *naturally* defined at these points because of a division by $a_k(s^*) = 0$. In [3], no indication was given regarding this matter. In [4], it was stated that "*[this] acceleration is not uniquely determined*" and suggested to choose *any* acceleration to initiate the integrations. In [5], [6] (and also in [16] which reproduced the reasoning of [5], [6]), the authors suggested to select the following acceleration to initiate the backward integration (and a similar expression for the forward integration):

$$\min(\alpha^-, \alpha^+, \alpha_{\mathrm{MVC}}), \text{ where} \tag{6}$$

$$\alpha^- = \lim_{s \uparrow s^*} \alpha(s, \mathrm{MVC}(s^*)), \tag{7}$$
$$\alpha^+ = \lim_{s \downarrow s^*} \alpha(s, \mathrm{MVC}(s^*)),$$

and α_{MVC} is computed from the *slope* of the MVC on the left of s^*.

However, observing the α-profiles near the dynamic singularity of Fig. 2A, it appears that the definition of α^- in equation (7) is arbitrary. Indeed, depending on the *direction* from which one moves towards $(s^*, \mathrm{MVC}(s^*))$ in the plane $(s, \dot{s})$ the limit of α is different: for instance, in Fig. 2A, if one moves from the top left, the limit, if it exists, would be positive, and it would be negative if one moves from the bottom left. In this context, the choice of equation (7) consisting of moving towards $(s^*, \mathrm{MVC}(s^*))$ *horizontally* is no more justified than any other choice. More generally, it is impossible to extend α by continuity towards $(s^*, \mathrm{MVC}(s^*))$ from the left because the α-profiles *diverge* when approaching $(s^*, \mathrm{MVC}(s^*))$ from the left. In fact, as we shall show in section IV, the only way to integrate α backward from $(s^*, \mathrm{MVC}(s^*))$ is to follow the "neutral" line, indicated by the black dashed line in Fig. 2A.

The above suggestion was first made in [9] in the particular case of time-optimal path parameterization with velocity and acceleration limits and paths made of straight segments and circular arcs. The authors observed that the "neutral" line was always horizontal and subsequently suggested to use 0 as the acceleration to initiate the backward and forward integrations from dynamic singularities.

As mentioned previously, we shall derive in section IV the analytic expression for the slope of the "neutral" line, which corresponds to the optimal forward and backward acceleration from dynamic singularities of type I. Furthermore, we shall show that the value of this acceleration is indeed 0 in the particular case considered in [9]. As for dynamic singularities of type II, the optimal backward and forward accelerations differ one from the other but can also be analytically determined.

III. CHARACTERIZING DYNAMIC SINGULARITIES

We first make a general assumption that there are no "degeneracies". An example of what we mean by "degeneracy" is when $a_i(s) = 0$ and $a_j(s) = 0$ with $i \neq j$ at the same point s. Indeed, while zero-inertia points occur in most real-world problem instances [6], the instances for which "there exists an s such that $a_i(s) = 0$ *and* $a_j(s) = 0$, with $i \neq j$" are extremely rare.

Throughout the rest of the development, we take the following convention.

Convention 1: Consider a zero-inertia point s^*, and assume that it is triggered by the k-th actuator, i.e. $a_k(s^*) = 0$. Since we have excluded degeneracies (in particular, the case of singular arcs [5] when $a_k = 0$ in an interval or the case when a_k is tangent to the line $\dot{s} = 0$), $a_k(s)$ must change sign at s^*. We take the convention that $a_k(s) > 0$ in a neighborhood to the left of s^* and $a_k(s) < 0$ in a neighborhood to the right of s^* (the case when a_k switches from negative to positive can be treated similarly by changing signs at appropriate places in the rest of the development).

We now prove the following proposition.

Proposition 1: If $\tau_k^{\min} - c_k(s^*) > 0$ or $\tau_k^{\max} - c_k(s^*) < 0$, then there exists a neighborhood $]s^* - \epsilon, s^* + \epsilon[$ such that $\mathrm{MVC}(s) = 0$ for all $s \in]s^* - \epsilon, s^* + \epsilon[$.

Proof: Suppose for instance that $\tau_k^{\min} - c_k(s^*) = \eta > 0$. By continuity of c_k, there exists a neighborhood $]s^* - \epsilon_1, s^* + \epsilon_1[$ such that

$$\forall s \in]s^* - \epsilon_1, s^* + \epsilon_1[, \ \tau_k^{\min} - c_k(s) > \eta/2.$$

Consider an arbitrary small ζ. Since $a_k(s^*) = 0$ and that $a_k(s) > 0$ in a neighborhood to the left of s^*, there exists a neighborhood $]s^* - \epsilon_2, s^*[$ such that

$$\forall s \in]s^* - \epsilon_2, s^*[,\ 0 < a_k(s) < \zeta.$$

Thus, we have

$$\forall s \in]s^* - \min(\epsilon_1, \epsilon_2), s^*[,\ \alpha(s,0) > \eta/(2\zeta),$$

where ζ can be chosen arbitrarily small.

Recall that $\alpha = \max_i \alpha_i$, thus by choosing a sufficiently small ζ, we can obtain a neighborhood where $\alpha(s,0) = \alpha_k(s,0)$. On the other hand, since $\beta = \min_i \beta_i$ and that the $\beta_i(s,0)$ where $i \neq k$ remain upper-bounded in a neighborhood of s^* (because $a_i(s) \neq 0$ for $i \neq k$), $\beta(s,0)$ is also upper-bounded in a neighborhood of s^*, say by a constant $K > 0$. It suffices now to chose a sufficiently small $\zeta < \eta/(2K)$ such that, for the corresponding $\epsilon = \min(\epsilon_1, \epsilon_2)$, we have

$$\forall s \in]s^* - \epsilon, s^*[,\ \alpha(s,0) > \beta(s,0).$$

The latter inequality implies by definition that $\mathrm{MVC}(s) = 0$ in that neighborhood.

For $s > s^*$, we can show using the same arguments as above that $\beta(s,0)$ is arbitrarily small near s^* while α is lower-bounded. The case $\tau_k^{\max} - c_k(s^*) < 0$ can also be proved by a similar reasoning $\square$

Convention 2: In light of Proposition 1, we assume from now on that $\tau_k^{\min} - c_k(s^*) < 0$ and $\tau_k^{\max} - c_k(s^*) > 0$.

Before proceeding further, let us define

$$\tilde{\alpha}_k(s,\dot{s}) = \max_{i \neq k} \alpha_i(s,\dot{s})$$

$$\tilde{\beta}_k(s,\dot{s}) = \min_{i \neq k} \beta_i(s,\dot{s}).$$

In other words, $\tilde{\alpha}_k$ and $\tilde{\beta}_k$ would be the acceleration limits, had the constraints associated with the k-th actuator been removed.

We now distinguish two cases according to the sign of $b_k(s^*)$.

A. Case $b_k(s^*) < 0$

From assumption 2 and the assumption that $b_k(s^*) < 0$, there exists $\eta > 0$ such that, in a neighborhood to the left of s^*

$$\forall \dot{s} \geq 0,\ \tau_k^{\max} - c_k(s) - b_k(s)\dot{s}^2 > \eta.$$

Thus, for any $K > 0$, there exists a neighborhood to the left of s^* where

$$\forall \dot{s} \geq 0,\ \beta(s,\dot{s}) > K.$$

By choosing a sufficiently large K, one can then obtain a neighborhood to the left of s^* in which $\beta(s,\dot{s}) = \tilde{\beta}_k(s,\dot{s})$ for all $\dot{s}$, that is, in which actuator k does not contribute to the *upper* acceleration limit.

Similarly, one can show that there exists a neighborhood to the *right* of s^* in which $\alpha(s,\dot{s}) = \tilde{\alpha}_k(s,\dot{s})$ for all $\dot{s}$, that is, in which actuator k does not contribute to the *lower* acceleration limit.

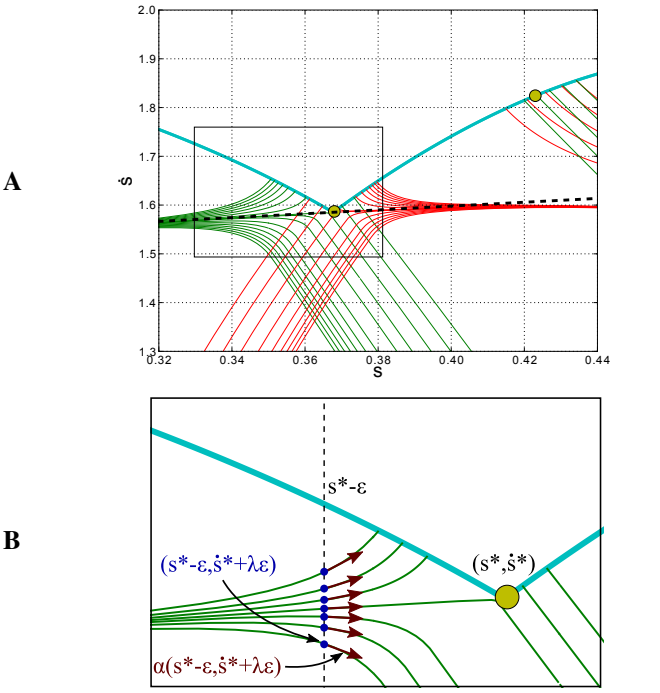

Fig. 2. **A**: α- and β-profiles (in green and red respectively) near zero-inertia points (yellow points). The leftmost zero-inertia point is an undifferentiable switch point of type I (cf. section III-A.2), while the rightmost zero-inertia point is not a dynamic singularity (cf. section III-A.1). Note that in agreement with the definitions, at any point in the plane the slope of the red profile is higher than the slope of the green profile, except on the MVC where the two slopes are equal. The dotted line is the line that goes through the switch point and has slope λ computed by equation (12) (cf. section IV). **B**: close-up view (zoomed in the black box of **A**) centered around the undifferentiable switch point.

Define next

$$\dot{s}^* = \sqrt{\frac{\tau_k^{\min} - c_k(s^*)}{b_k(s^*)}}. \tag{8}$$

Recall from our assumptions that the expression under the radical sign is indeed positive. Let $\tilde{\dot{s}}^*$ be the smallest velocity $\dot{s}$ which satisfies ($\tilde{\dot{s}}^* = +\infty$ if no such $\dot{s}$ exists)

$$\tilde{\alpha}_k(s^*,\dot{s}) = \tilde{\beta}_k(s^*,\dot{s}). \tag{9}$$

In other words, $\tilde{\dot{s}}^*$ would be the value of the MVC at s^*, had the constraints associated with the k-th actuator been removed.

We now distinguish two sub-cases.

1) Sub-case $\tilde{\dot{s}}^* < \dot{s}^*$: Let $\dot{s}_m = (\tilde{\dot{s}}^* + \dot{s}^*)/2$. By the definition of $\dot{s}^*$ and the assumption that $b_k(s^*) < 0$, there exists $\eta > 0$ such that, in a neighborhood to the left of s^*

$$\forall \dot{s} \leq \dot{s}_m,\ \tau_k^{\min} - c_k(s) - b_k(s)\dot{s}^2 < -\eta.$$

By the same argument as above, one can then show that there exists a neighborhood to the *left* of s^* in which $\alpha(s,\dot{s}) = \tilde{\alpha}_k(s,\dot{s})$ for all $\dot{s} \leq \dot{s}_m$, that is, in which actuator k does not contribute to the *lower* acceleration limit.

Similarly, one can show that there exists a neighborhood to the *right* of s^* in which $\beta(s,\dot{s}) = \tilde{\beta}_k(s,\dot{s})$ for all $\dot{s} \leq \dot{s}_m$,

that is, in which actuator k does not contribute to the *upper* acceleration limit.

In summary, there exists a neighborhood $]s^* - \epsilon, s^* + \epsilon[$ such that

$$\forall (s, \dot{s}) \in]s^* - \epsilon, s^* + \epsilon[\times [0, \dot{s}_m], \ \begin{cases} \alpha(s, \dot{s}) = \tilde{\alpha}_k(s, \dot{s}) \\ \beta(s, \dot{s}) = \tilde{\beta}_k(s, \dot{s}). \end{cases} \quad (10)$$

Since $\tilde{\dot{s}} < \dot{s}_m$, the definition of $\tilde{\dot{s}}^*$ in equation (9) implies that

$$\alpha(s^*, \tilde{\dot{s}}^*) = \beta(s^*, \tilde{\dot{s}}^*),$$

which implies in turn that $\mathrm{MVC}(s^*) = \tilde{\dot{s}}^*$.

Furthermore, from equation (10), the behavior of the MVC in the interval $]s^* - \epsilon, s^* + \epsilon[$ is fully characterized by $\tilde{\alpha}_k$ and $\tilde{\beta}_k$, which contain no singularity in this interval (further restrict the interval if necessary). One can thus conclude that the MVC is *continuous and differentiable* around s^* and that α and β are well-defined and equal on the MVC (see Fig. 2A), which in turn implies that, in this sub-case, s^* is *not* a dynamic singularity.

2) Sub-case $\tilde{\dot{s}}^* > \dot{s}^*$: Since the β_i where $i \neq k$ do not involve any singularity around s^*, there exists a neighborhood around $(s^*, \dot{s}^*)$ where $\tilde{\beta}_k$ is given by β_p for a fixed $p \neq k$. Furthermore, since we have remarked at the beginning of section III-A that in a neighborhood to the left of s^*, one has $\beta = \tilde{\beta}_k$, one actually has $\beta = \beta_p$ in a neighborhood to the left of s^*.

Let next

$$u(s) = \frac{a_k(s)[\tau_p^\beta - c_p(s)] - a_p(s)[\tau_k^{\min} - c_k(s)]}{a_k(s)b_p(s) - a_p(s)b_k(s)}.$$

Note that, if $u(s) \geq 0$, then $\dot{s} = \sqrt{u(s)}$ satisfies $\alpha_k(s, \dot{s}) = \beta_p(s, \dot{s})$. From the fact that $a_k(s^*) = 0$, one has

$$\lim_{s \uparrow s^*} u(s) = \frac{\tau_k^{\min} - c_k(s^*)}{b_k(s^*)} = \dot{s}^{*2}.$$

Thus, there exists a neighborhood to the left of s^* where $0 < u(s) < \tilde{\dot{s}}^{*2}$ (the second inequality comes from our assumption that $\tilde{\dot{s}}^* > \dot{s}^*$). We argue that, in that neighborhood, $\mathrm{MVC}(s) = \sqrt{u(s)}$. Indeed, as remarked above, $\sqrt{u(s)}$ satisfies $\alpha_k(s, \sqrt{u(s)}) = \beta_p(s, \sqrt{u(s)})$. Furthermore, if $i \neq k$, there is no $\dot{s} < \sqrt{u(s)}$ that satisfies $\alpha_i(s, \dot{s}) = \beta_p(s, \dot{s})$ since $\sqrt{u(s)} < \tilde{\dot{s}}^*$ and by definition of $\tilde{\dot{s}}^*$.

As a consequence, one also has $\alpha = \alpha_k$ in that neighborhood.

Regarding the *right* of s^*, following a similar reasoning as above, one first determines $q \neq k$ such that $\alpha_q = \tilde{\alpha}_k$ in a neighborhood to the right of s^*. Consider then

$$v(s) = \frac{a_k(s)[\tau_q^\alpha - c_q(s)] - a_q(s)[\tau_k^{\min} - c_k(s)]}{a_k(s)b_q(s) - a_q(s)b_k(s)}.$$

Note that we have indeed written $\tau_k^{\min}$ (and not $\tau_k^{\max}$) in the above equation, since $a(s) < 0$ to the right of s^*. Next, one can show similarly as above that there exists a neighborhood to the right of s^* in which $\mathrm{MVC}(s) = \sqrt{v(s)}$ and, as a consequence, in which $\beta = \beta_k$

Combining the results concerning the left and the right of $\dot{s}$, one obtains that the MVC is *continuous* at s^*, since

$$\lim_{s \uparrow s^*} \sqrt{u(s)} = \lim_{s \downarrow s^*} \sqrt{v(s)} = \dot{s}^*.$$

However, the MVC is *undifferentiable* at s^* since, in general,

$$\lim_{s \uparrow s^*} \left(\sqrt{u(s)}\right)' \neq \lim_{s \downarrow s^*} \left(\sqrt{v(s)}\right)'.$$

Thus, in this sub-case, s^* is indeed a dynamic singularity – which we label as "of type I" – and therefore a candidate undifferentiable switch point.

B. Case $b_k(s^*) > 0$

From assumption 2 and the assumption that $b_k(s^*) \geq 0$, one has that $\tau_k^{\min} - c_k(s^*) - b_k(s^*)\dot{s}^2 < 0$ for all $\dot{s}$. Thus, there exists a neighborhood $]s^* - \epsilon, s^*[$ where $\alpha_k(s, \dot{s})$ is arbitrary small, in such a way that

$$\forall s \in]s^* - \epsilon, s^*[, \ \forall \dot{s}, \ \alpha(s, \dot{s}) = \tilde{\alpha}_k(s, \dot{s}) = \alpha_p(s, \dot{s}),$$

for some $p \neq k$. Similarly, one has on the right of s^*

$$\forall s \in]s^*, s^* + \epsilon[, \ \forall \dot{s}, \ \beta(s, \dot{s}) = \tilde{\beta}_k(s, \dot{s}) = \beta_q(s, \dot{s}),$$

for some $q \neq k$.

The crucial change with respect to case $b_k(s^*) < 0$ is that here α, not β, is well-defined and smooth on the *left* of s^*. Since the *backward* integration uses α, we simply initiate using the value $\alpha_p(s^*, \mathrm{MVC}(s^*))$. Similarly, to initiate the forward integration, we use the value $\beta_q(s^*, \mathrm{MVC}(s^*))$.

Define next

$$\dot{s}^* = \sqrt{\frac{\tau_k^{\max} - c_k(s^*)}{b_k(s^*)}}. \quad (11)$$

Note from our assumptions that the expression under the radical sign is indeed positive. Let $\tilde{\dot{s}}^*$ be the smallest velocity $\dot{s}$ which satisfies equation (9) ($\tilde{\dot{s}}^* = +\infty$ if no such $\dot{s}$ exists).

Using the same arguments as in case $b_k(s^*) < 0$, one can show that

- If $\tilde{\dot{s}}^* < \dot{s}^*$, the MVC is continuous and differentiable at s^*, which therefore is not a switch point;
- If $\tilde{\dot{s}}^* > \dot{s}^*$, the MVC is continuous but undifferentiable at s^*. Thus s^* is a dynamic singularity – which we label as "of type II" – and therefore a candidate undifferentiable switch point.

IV. ADDRESSING DYNAMIC SINGULARITIES

A. Addressing Dynamic Singularities of Type I

Fig. 2B shows in more detail the α-profiles near a singular switch point s^* of type I. Note first that, according to section III-A.2, α is given by α_k in a neighborhood to the left of s^*, and β is given by β_k in a neighborhood to the right of s^*.

Next, note that the α-profiles are divergent as they approach $(s^*, \dot{s}^*)$ from the left. Thus, one cannot naturally extend α_k by continuity to $(s^*, \dot{s}^*)$ from the left.

Consider the intersections of the vertical line $s = s^* - \epsilon$, where ϵ is an arbitrary small positive number, with the α-profiles. An α-profile can reach $(s^*, \dot{s}^*)$ only if its *tangent vector* at the intersection *points towards* $(s^*, \dot{s}^*)$. This can be achieved if there exists a real number λ such that

$$\frac{\alpha_k(s^* - \epsilon, \dot{s}^* + \lambda\epsilon)}{\dot{s}^* + \lambda\epsilon} = \lambda.$$

Replacing α_k by its expression yields the condition

$$\frac{\tau_k^{\min} - c_k(s^* - \epsilon) - b_k(s^* - \epsilon)(\dot{s}^* + \lambda\epsilon)^2}{a_k(s^* - \epsilon)(\dot{s}^* + \lambda\epsilon)} = \lambda, \text{ i.e.}$$

$$\tau_k^{\min} - c_k(s^* - \epsilon) - b_k(s^* - \epsilon)(\dot{s}^* + \lambda\epsilon)^2 = \lambda(\dot{s}^* + \lambda\epsilon)a_k(s^* - \epsilon).$$

Computing the Taylor expansion of the above equation at order 1 in ϵ and recalling that $\tau_k^{\min} - c_k(s^*) - b_k(s^*)\dot{s}^{*2} = 0$ and $a_k(s^*) = 0$, one obtains the condition

$$c_k'(s^*) + b_k'(s^*)\dot{s}^{*2} - 2\lambda b_k(s^*)\dot{s}^* = \lambda \dot{s}^* a_k'(s^*).$$

Solving for λ, one finally obtains

$$\lambda = -\frac{c_k'(s^*) + b_k'(s^*)\dot{s}^{*2}}{[2\lambda b_k(s^*) + a_k'(s^*)]\dot{s}^*}. \tag{12}$$

Following the same reasoning on the right of s^*, one has to solve

$$\frac{\beta_k(s^* + \epsilon, \dot{s}^* + \lambda\epsilon)}{\dot{s}^* + \lambda\epsilon} = -\lambda,$$

which leads to the same value as in equation (12). Thus the optimal backward and forward acceleration at $(s^*, \dot{s}^*)$ is given by equation (12). One can observe in Fig. 2A that the black dotted line, whose slope is given by λ, indeed constitutes the "neutral" line at $(s^*, \dot{s}^*)$.

B. Algorithm and Simulations

Based on the results obtained so far, we propose the following algorithm when encountering a zero-inertia point s^*, with $a(s^*) > 0$ on the left of s^* and $a(s^*) < 0$ on the right of s^*:

1) If $b_k(s^*) < 0$: compute $\dot{s}^*$ by equation (8) and $\tilde{\dot{s}}^*$ by solving equation (9).

- If $\dot{s}^* > \tilde{\dot{s}}^*$, then s^* is not a dynamic singularity, therefore not a candidate switch point.
- If $\dot{s}^* < \tilde{\dot{s}}^*$, then s^* is a dynamic singularity of type I. Next, compute λ by equation (12).
  - Integrate the constant field $(\dot{s}^*, \lambda\dot{s}^*)$ *backward* for a small number of time steps. Then continue by following α, as in the original algorithm;
  - Integrate the constant field $(\dot{s}^*, \lambda\dot{s}^*)$ *forward* for a small number of time steps. Then continue by following β.

2) If $b_k(s^*) > 0$: compute $\dot{s}^*$ by equation (11) and $\tilde{\dot{s}}^*$ by solving equation (9).

- If $\dot{s}^* > \tilde{\dot{s}}^*$, then s^* is not a dynamic singularity, therefore not a candidate switch point.
- If $\dot{s}^* < \tilde{\dot{s}}^*$, then s^* is a dynamic singularity of type II. If $\tilde{\alpha}_k(s, \dot{s})$ or $\tilde{\beta}_k(s, \dot{s})$ "traverses" the MVC then s^* is not a switch point. Otherwise,
  - Integrate $\tilde{\alpha}_k(s, \dot{s})$ backward for a small number of time steps. Then continue by following α, as in the original algorithm;
  - Integrate $\tilde{\beta}_k(s, \dot{s})$ forward for a small number of time steps. Then continue by following β.

Note that after integrating a small number of steps away from s^*, the fields α and β become smooth, so that there is no problem of singularity.

We applied the above algorithm on a dynamic model of the 4-dof Barrett WAM using the OpenRAVE robotic simulation platform [17]. The torque limits were set at $\pm 6\,\text{N·m}$, $\pm 15\,\text{N·m}$, $\pm 5\,\text{N·m}$, $\pm 4\,\text{N·m}$ respectively for the shoulder yaw, pitch and roll joints and the elbow joint. The results show a smooth behaviour around the undifferentiable switch point, both for the $(s, \dot{s})$ profile and for the torque profiles, see Fig. 3.

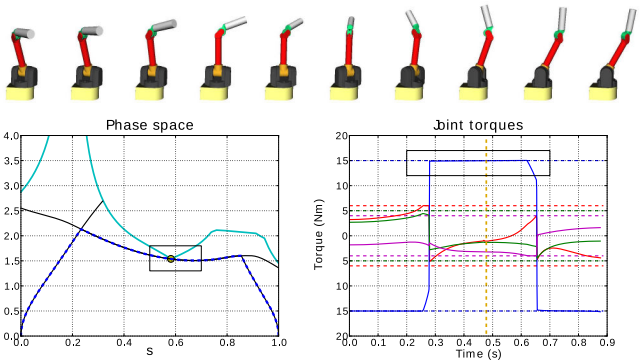

Fig. 3. Simulations for a 4-link manipulator. **Top**: snapshots of the time-parameterized trajectory taken every 10% of trajectory duration. **Left**: $(s, \dot{s})$ space. Same legends as in Fig. 2. The superimposed dotted blue line indicates the final $(s, \dot{s})$ profile, which follows parts of the computed α- and β-profiles (black). **Right**: torque profiles. The torques for the shoulder yaw, pitch, roll and elbow joints were plotted in red, blue, green and magenta respectively. The torque limits are indicated by horizontal dotted lines. Note that, in agreement with time-optimal control theory, at least one torque limit is saturated at any time instant. The vertical dotted yellow line indicates the time instant of the zero-inertia point.

Next, to illustrate more clearly the improvements permitted by our algorithm, we compared the results given by our algorithm and that given by the algorithm of [5], [6], which use unsatisfactory values for the accelerations at dynamic singularities. The results suggest that, in the numerical integration of the $(s, \dot{s})$ profiles, the algorithm of [5] needed to use a time step at least 5 times finer (corresponding thus to an execution time potentially 5 times longer) than our algorithm to achieve the same precision, see Fig. 4.

C. About Kunz and Stilman's Conjecture

Kunz and Stilman [9] were first to remark – in the particular case of time-optimal path parameterization with velocity and acceleration limits and paths made of straight segments and circular arcs – that the algorithm proposed in [5], [6] could not satisfactorily address all dynamic singularities. From equation (14) of [9], the correspondences between the parameters of [9] and those of the present article are given in Table I.

Remark next that the zero-inertia points in [9] are all located in the circular portions. In such portions, the coefficients a_k and b_k have the following form (using our notations):

$$\begin{aligned} a_k(s) &= -\frac{C_1}{r}\sin\left(\frac{s}{r}\right) + \frac{C_2}{r}\cos\left(\frac{s}{r}\right), \\ b_k(s) &= \frac{C_1}{r^2}\cos\left(\frac{s}{r}\right) - \frac{C_2}{r^2}\sin\left(\frac{s}{r}\right), \end{aligned}$$

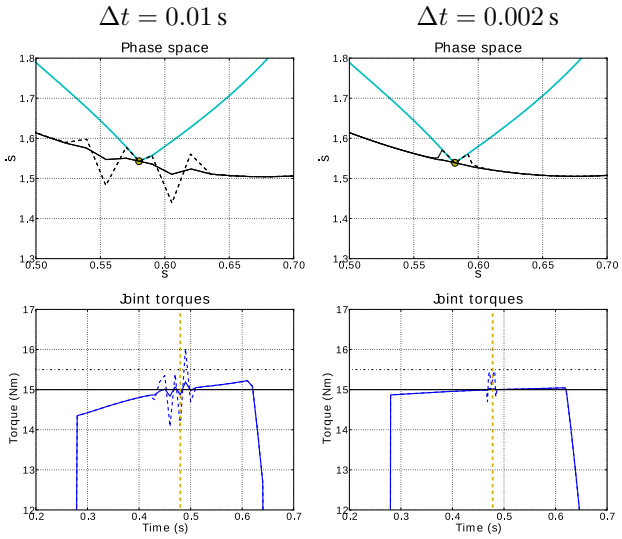

Fig. 4. Close-up views (zoomed in the black boxes of Fig. 3) of the $(s, \dot{s})$ profiles and of the shoulder pitch torque profiles around the switch point, computed using two different integration time steps Δt. Solid lines: results of our algorithm, dotted lines: results of the algorithm proposed by [5]. The vertical dotted yellow line indicates the time instant of the zero-inertia point. Note that our algorithm yielded torques that were within the $+0.5\,\mathrm{N{\cdot}m}$ tolerance even for $\Delta t = 0.01$ while the algorithm of [5] needed to use $\Delta t = 0.002$ (5 times finer) to get within the same tolerance.

TABLE I

PARAMETERS CORRESPONDENCES

This article		Kunz and Stilman [9]
$(\tau_k^{\min}, \tau_k^{\max})$	$\leftrightarrow$	$(-\ddot{q}_k^{\max}, \ddot{q}_k^{\max})$
$a_k(s)$	$\leftrightarrow$	$f_k'(s)$
$b_k(s)$	$\leftrightarrow$	$f_k''(s)$
$c_k(s)$	$\leftrightarrow$	0

where C_1 and C_2 are two constants independent of s. Differentiating b_k next yields

$$b_k'(s) = -\frac{C_1}{r^3}\sin\left(\frac{s}{r}\right) + \frac{C_2}{r^3}\cos\left(\frac{s}{r}\right) = \frac{1}{r^2}a_k(s).$$

One thus has $b_k'(s^*) = 1/r^2 a_k(s^*) = 0$ at a zero-inertia point. If this zero-inertia point is actually an undifferentiable switch point of type I then, from equation (12), one obtains that $\lambda = 0$, which corresponds to the conjecture made in [9].

V. CONCLUSION

By studying closely the minimum and maximum acceleration profiles in the vicinities of dynamic singularities, we have obtained a complete characterization of such singularities, which play a critical role in the classic TOPP algorithm. In the process, we have also established a general classification of switch points and related notions associated with this important algorithm.

On the practical side, we have shown how to address dynamic singularities, which allows making the TOPP algorithm more robust to discretization errors. In light of the simulations of Fig. 4, one could also use a variable-time-step integration scheme whereby the time step would be refined near zero-inertia points to achieve a good precision, without ever using the correct acceleration of equation (12). However, such a method would be cumbersome and would lack the elegance and the correctness of the solution presented here.

We are currently working on extending the method of analysis developed here to address dynamic singularities arising in other variations of the TOPP algorithm, such as in [7], [8], [10].

ACKNOWLEDGMENT

This work was completed when the author was with Department of Mechano-Informatics, University of Tokyo, Japan, and was supported by a JSPS postdoctoral fellowship. We thank Prof. Z. Shiller, Prof. Y. Nakamura, S. Caron and T. Kunz for many valuable discussions.

REFERENCES

[1] J. Bobrow, S. Dubowsky, and J. Gibson, "Time-optimal control of robotic manipulators along specified paths," *The International Journal of Robotics Research*, vol. 4, no. 3, pp. 3–17, 1985.

[2] K. Shin and N. McKay, "Minimum-time control of robotic manipulators with geometric path constraints," *IEEE Transactions on Automatic Control*, vol. 30, no. 6, pp. 531–541, 1985.

[3] F. Pfeiffer and R. Johanni, "A concept for manipulator trajectory planning," *IEEE Journal of Robotics and Automation*, vol. 3, no. 2, pp. 115–123, 1987.

[4] J. Slotine and H. Yang, "Improving the efficiency of time-optimal path-following algorithms," *IEEE Transactions on Robotics and Automation*, vol. 5, no. 1, pp. 118–124, 1989.

[5] Z. Shiller and H. Lu, "Computation of path constrained time optimal motions with dynamic singularities," *Journal of dynamic systems, measurement, and control*, vol. 114, p. 34, 1992.

[6] Z. Shiller, "On singular time-optimal control along specified paths," *IEEE Transactions on Robotics and Automation*, vol. 10, no. 4, pp. 561–566, 1994.

[7] Z. Shiller and S. Dubowsky, "Robot path planning with obstacles, actuator, gripper, and payload constraints," *The International Journal of Robotics Research*, vol. 8, no. 6, pp. 3–18, 1989.

[8] Z. Shiller and Y. Gwo, "Dynamic motion planning of autonomous vehicles," *IEEE Transactions on Robotics and Automation*, vol. 7, no. 2, pp. 241–249, 1991.

[9] T. Kunz and M. Stilman, "Time-optimal trajectory generation for path following with bounded acceleration and velocity," in *Robotics: Science and Systems*, vol. 8, 2012, pp. 09–13.

[10] Q.-C. Pham and Y. Nakamura, "Time-optimal path parameterization for critically dynamic motions of humanoid robots," in *IEEE-RAS International Conference on Humanoid Robots*, 2012.

[11] J. Bobrow, "Optimal robot plant planning using the minimum-time criterion," *IEEE Journal of Robotics and Automation*, vol. 4, no. 4, pp. 443–450, 1988.

[12] Z. Shiller and S. Dubowsky, "On computing the global time-optimal motions of robotic manipulators in the presence of obstacles," *IEEE Transactions on Robotics and Automation*, vol. 7, no. 6, pp. 785–797, 1991.

[13] Q.-C. Pham, "Planning manipulator trajectories under dynamics constraints using minimum-time shortcuts," in *Second IFToMM ASIAN Conference on Mechanism and Machine Science*, 2012.

[14] Q.-C. Pham, S. Caron, and Y. Nakamura, "Kinodynamic planning in the configuration space via velocity interval propagation," *Robotics: Science and System*, 2013.

[15] B. Goodwine and J. Nightingale, "The effect of dynamic singularities on robotic control and design," in *IEEE International Conference on Robotics and Automation*, 2010, pp. 5213–5218.

[16] H. Choset, K. M. Lynch, S. Hutchinson, G. Kantor, W. Burgard, L. E. Kavraki, and S. Thrun, *Principles of robot motion: theory, algorithms, and implementations*. MIT press, 2005.

[17] R. Diankov, "Automated construction of robotic manipulation programs," Ph.D. dissertation, Carnegie Mellon University, Robotics Institute, August 2010. [Online]. Available: http://www.programmingvision.com/rosen_diankov_thesis.pdf